Available online at www.sciencedirect.com
SCIENCE DIRECT®
PERGAMON
Deep-Sea Research I 50 (2003) 131–150
DEEP-SEA RESEARCH PART I
www.elsevier.com/locate/dsr

Abundance, distribution and sinking rates of aggregates in the Ross Sea, Antarctica

Vernon L. Asper[a,*], Walker O. Smith Jr.[b]

[a] College of Marine Sciences, University of Southern Mississippi, Stennis Space Center, MS 39529, USA
[b] Virginia Institute of Marine Science, College of William and Mary, Gloucester Pt., VA 23062, USA

Received 24 January 2002; received in revised form 4 November 2002; accepted 8 November 2002

Abstract

The vertical distribution and temporal changes in aggregate abundance and sizes were measured in the Ross Sea, Antarctica, during two field seasons, one in austral spring 1994 and one in early summer, 1995/96. Aggregate abundance, size and potential sinking rates were determined by photographic techniques. Measurements of water column parameters, including particulate organic carbon concentrations, were assessed simultaneously, as was the flux of organic matter with floating sediment traps. The numbers of aggregates (and to a lesser extent their size) increased with time, although there was substantial spatial variability in these variables at any point in time. Some aggregates appeared to sink extremely rapidly, and for these, our photographic measurements were able to estimate only a minimum sinking rate, which equaled 288 m d^{-1}. Estimates of aggregate organic carbon flux were compared to those determined by floating sediment traps. From these results, aggregate fluxes appear to have dominated the vertical export of organic matter from the euphotic zone. The genesis and flux of aggregates in the Ross Sea are the critical processes controlling the export of biogenic material from the surface layer.

Keywords: Aggregates; Aggregation; Antarctic zone; Phytoplankton; *Phaeocystis*; Ross Sea

1. Introduction

The Ross Sea represents the largest area of elevated pigment concentrations in the Antarctic, being the site of intense phytoplankton blooms during austral spring and summer. Much of the carbon that is utilized by the food web is produced during these blooms, and therefore they are critical contributors to food web dynamics of the region. Although it has been shown that an intense bloom develops in the southern Ross Sea by January (Smith and Nelson, 1985; Arrigo and McClain, 1994; Arrigo et al., 1999), questions about the fate and transformation of this material remain. Our understanding remains limited regarding the controls of the bloom, the fate of the bloom products or the role of this region in contemporary or historical global elemental cycles.

One important feature affecting productivity in this region is the formation of the Ross Sea Polynya. The polynya (an area of reduced ice cover surrounded by concentrated ice) forms in

*Corresponding author. Tel.: +1-228-688-3178; fax: +1-228-688-1121.
E-mail address: vernon.asper@usm.edu (V.L. Asper).

0967-0637/03/$ - see front matter
doi:10.1016/S0967-0637(02)00146-2

austral spring at the edge of the Ross Ice Shelf and progressively expands northwards from November through January (Zwally et al., 1983; Comiso et al., 1993). The polynya is generated by two factors (Jacobs and Comiso, 1991; Markus, 1999). The first is that southerly winds blow from the ice shelf and onto the pack ice, advecting the ice northward and exposing open water. The exposed seawater freezes quickly and is in turn driven north by the wind and the prevailing cyclonic circulation, thickening as it ages and moves. The second factor that initiates and sustains the polynya is the advection of warm ($\approx -0.5°C$), Antarctic Circumpolar Current water onto the shelf from the continental slope. This warm water thus provides a heat source and aids in melting the ice. It is likely that both processes are operating in generating the Ross Sea Polynya (Jacobs and Comiso, 1991; Markus, 1999). The large expansion in late spring is largely driven by a positive heat budget for the region. The dynamics of the polynya, in turn, control the phytoplankton blooms in the Ross Sea (Smith and Nelson, 1985; Arrigo et al., 1998), which are responsible for the production and export of large amounts of particulate matter over short time intervals (Asper and Smith, 1999).

The Ross Sea is characterized by blooms of diatoms and of the colonial haptophyte *Phaeocystis antarctica* (Smith et al., 1996; DiTullio and Smith, 1996; Arrigo et al., 1999; Smith and Asper, 2001). These blooms result in massive accumulations of biogenic material in the upper water column (e.g., biogenic silica and particulate organic carbon (POC) concentrations >60 and $85\,\mu mol\,l^{-1}$, respectively; Smith and Nelson, 1985; Smith et al., 1996). The blooms of *P. antarctica* are also notable for the significant amounts of organic matter that is partitioned into the alga's mucoid sheath (Mathot et al., 2000). Much of the material produced during the early part of the bloom accumulates in the upper water column, but particulate organic matter concentrations begin to decrease in mid-January, despite the favorable irradiance and macronutrient regime (Asper and Smith, 1999; Smith et al., 2000). Although export via fecal pellets can be substantial (Gowing et al., 2001), losses from the surface layer resulting from grazing by meso- or microzooplankton have been shown to be minimal throughout the summer over much of the southern Ross Sea (Caron et al., 2000). It has been suggested that the losses of particulate matter are mediated by aggregate formation and rapid vertical flux of large particles (Asper and Smith, 1999; Gardner et al., 2000), but this remains unverified.

The importance of aggregate formation and subsequent enhanced vertical flux have been successfully modeled (e.g., Jackson, 1990; Jackson and Lochmann, 1992; Riebesell and Wolf-Gladrow, 1992; Jackson, 1995). These results suggest that aggregation under high biomass conditions can be a critical factor in reducing the organic matter load of the surface layer through the production of large particles that sink rapidly from the surface layer. The processes and factors that control the formation of aggregates have been experimentally investigated (e.g., Kiørboe and Hansen, 1993; Passow et al., 1994; Waite et al., 1997). Aggregate production is generally thought to be a function of particle concentration, stickiness, interactions with transparent exopolymer particles, and the number of collisions between particles. Stickiness in turn appears to be biologically controlled, and it is often thought to increase upon the onset of nutrient limitation (Kiørboe et al., 1990). However, mesocosm studies showed that increases in stickiness occur in diatoms *prior* to nutrient depletion (Alldredge et al., 1995). Furthermore, stickiness is a function of species composition. For example, Passow et al. (1994) found that temperate diatoms were much "stickier" than either phytoflagellates or *Phaeocystis* sp. Similarly, Waite et al. (1997) found a distinct gradient in stickiness that was related to the species composition of natural assemblages. Stickiness was correlated with the production of aggregates and disappearance of species from the water column, and thus reinforced the potential importance of aggregate formation as a loss process.

Aggregates occur throughout the ocean, and their composition and concentration vary tremendously. They can form from the coagulation of smaller particles (Jackson, 1990), the release of zooplankton structural bodies (Alldredge and

Cox, 1982), or a combination of the two. They are substantially larger than the median particle present in the surface layer, and harbor a community that results in a microenvironment within the surface layer (Alldredge and Cox, 1982). Sampling aggregates with Niskin bottles is generally unsuccessful because of their fragile nature, and novel techniques have been used to sample these particles and quantify their concentrations (e.g., collection by divers, Alldredge, 1998; high resolution in situ photography, Honjo et al., 1984). Despite an increase in our knowledge of the role of aggregates to upper ocean particle transformations, we still lack a quantitative understanding of their role in many oceanic biogeochemical cycles (Riebesell, 1993). Similarly, although the role of aggregates in carbon cycling in polar systems has been suggested, few studies have quantified the abundance and sinking rates of aggregates and the relationship of both to environmental factors. This paper reports the results of an investigation into the abundance, distribution and sinking rate of aggregates in the Ross Sea (Antarctica) polynya, and the temporal patterns and environmental controls of each.

2. Materials and methods

Two cruises on the *R.V.I.B. Nathaniel B. Palmer* were completed to the southern Ross Sea, Antarctica (Fig. 1). The first was conducted during austral spring (Cruise NBP94-06, November 10–December 8, 1994) and the second during the late spring-early summer period (Cruise NBP95-08, December 10, 1995–January 10, 1996). During the spring cruise a total of 77 stations were sampled for water column properties, and during the summer cruise data were collected at 92 stations (Smith and Asper, 2001). Sampling concentrated on a section along 76°30′S (stations spaced 60 km apart), and this transect was re-occupied during both cruises (two times in 1994, and three times in 1995/96). In addition, transects were occupied along 75°S and 173°E in 1994, and in 1995/96 along 172°E, to obtain additional information on the spatial variations in hydrography and phytoplankton.

Hydrographic data and water samples were collected with a Sea-Bird 911+CTD and 24 10-l Niskin bottles mounted on a Teflon-coated rosette (Smith and Asper, 2001). Spatial and temporal variations in POC concentrations, particle and aggregate abundance, sinking rates, contributions to vertical flux, and qualitative composition in the Ross Sea were also determined on both cruises. POC concentrations were determined by high temperature pyrolysis. Samples were filtered through pre-combusted GF/F filters under low vacuum, rinsed with 0.01 N HCl in seawater, and dried at 60°C (Smith and Asper, 2001). Concentrations of particulate matter (small particles, mostly $<20\,\mu m$ in diameter, Chung et al., 1996) were quantified with a SeaTech 25 cm path-length transmissometer attached to the rosette system. To calibrate the instrument, large volumes (ca. 10 liters) of water were acquired during the transmissometer cast and filtered through pre-weighed, 0.45 μm, 47 mm diameter membrane filters (Gardner et al., 2000). All filters were rinsed (Milli-Q water) inside a laminar flow hood, placed in sealed petri dishes, dried at 60°C, and weighed on an electrobalance. These data were related to POC measurements that were made on separate casts to allow interpolation between depths where actual POC determinations were made, and it was assumed that the relationship between POC and beam attenuation (c) is constant with depth. Stations were grouped by time of sampling into three groups to remove any marked temporal trends. The relationship was linear in all cases, and all regressions were significant at $p<0.001$. R^2 values were 0.74, 0.85 and 0.90 for the three periods.

2.1. Aggregate abundance and distribution

The abundance and distribution of aggregates was determined photographically (Honjo et al., 1984) with the MArine AGgregate ENUMerator (MAGENUM). This system incorporates a collimated strobe system and a 35 mm film camera (Lobsiger Deepslope 6000) mounted on an aluminum frame which was lowered slowly through the water column, acquiring six images min^{-1} throughout the entire water column. The

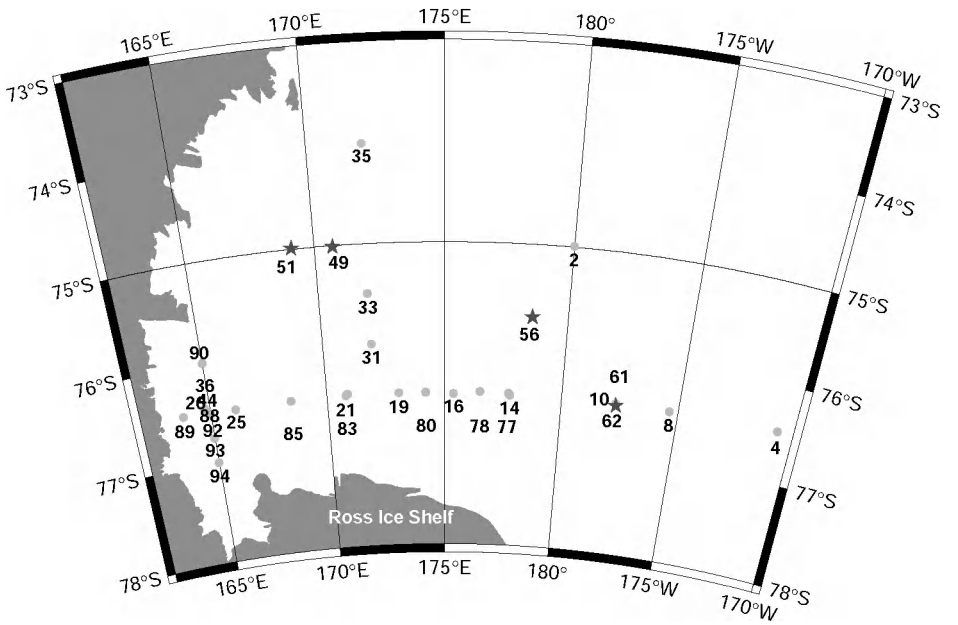

Fig. 1. Map of the study region showing the locations of the ROV (★ 1994) and MAGENUM (● 1995–1996) deployments in the Ross Sea.

illumination system consists of a pair of light heads (Deep Sea Power and Light) that are positioned facing each other to produce a narrow (9 cm deep) beam of uniform, collimated illumination 66 cm from the camera lens. Aggregates larger than 0.2 mm within this volume (15 liters) appear on photographs taken by a camera that is oriented perpendicular to the long axis of the beam of light, and can therefore be distinguished and characterized by computer analysis. Ambient light interferes with this process, so that profiles were obtained near midnight whenever possible to minimize this effect (24-h photoperiods occurred throughout both cruises). To record the depth of each photograph and collect hydrographic data for each camera cast, a Sea-Bird Seacat CTD and 25 cm SeaTech transmissometer were mounted on the camera frame. During the 1994 cruise we experienced technical difficulties with this system but were able to collect limited data using a similar system mounted on an R.O.V., and using a Benthos 873 camera. This system used the same illumination system, film, and lens (Nikonos 35 mm) so that, although no direct intercalibrations are available, it can be reasonably assumed that the results are comparable. A listing of locations and dates sampled in both years is provided in Table 1.

Except for short sections of film developed at sea to evaluate system function, all film was returned to the laboratory for processing. The films were developed and digitized commercially, yielding 3072×2944 images (Kodak PCD format) which were analyzed in our lab with Image Pro Plus software, with a final resolution of the digitized images of 5.2 pixels per mm. In order to insure that the same portion of each image was analyzed, an area of interest (AOI) was created in the region of maximum and most consistent illumination. This AOI was then carefully positioned to the same location within each image before particles were counted. Images were calibrated with a measuring tape included in each image for this purpose, and only objects larger than 0.5 mm were recorded, to be consistent with the generally accepted lower size limit of marine snow (Alldredge and Silver, 1988). Measurements performed included length, width, maximum

Table 1
Location of stations in the Ross Sea where aggregate profiles were collected

Station no.	Latitude (°S)	Longitude (°)	Date	Type of cast
49	75.01	170.71 E	28-Nov-94	ROV-1
51	74.99	169.12 E	29-Nov-94	ROV-4
56	75.72	178.55 E	1-Dec-94	ROV-6
62	76.52	177.67 W	2-Dec-94	ROV-8
2	74.99	179.99 E	20-Dec-95	MAG-1
4	76.47	170.69 W	22-Dec-95	MAG-2A
8	76.50	175.37 W	22-Dec-95	MAG-2B
10	76.50	177.69 W	23-Dec-95	MAG-3
14	76.50	177.76 E	23-Dec-95	MAS-1D
14	76.51	177.79 E	24-Dec-95	MAG-4
16	76.51	175.39 E	24-Dec-95	MAG-5
17	76.34	177.68 E	26-Dec-95	MAS-1R
19	76.49	173.06 E	26-Dec-95	MAG-7
21	76.50	170.76 E	27-Dec-95	MAS-2D
21	76.49	170.80 E	27-Dec-95	MAG-8
25	76.51	166.07 E	28-Dec-95	MAG-9
26	76.50	164.91 E	29-Dec-95	MAG-10
28	76.49	171.52 E	30-Dec-95	MAS-2R
31	76.00	172.00 E	30-Dec-95	MAG-11
33	75.50	171.94 E	30-Dec-95	MAG-12
35	74.01	172.02 E	31-Dec-95	MAG-13
36	76.50	164.97 E	1-Jan-96	MAS-3D
36	76.51	164.99 E	1-Jan-96	MAG-14
37A	77.66	165.98 E	2-Jan-96	MAG-15
40	76.46	164.97 E	3-Jan-96	MAS-3R
44	76.50	164.96 E	3-Jan-96	MAG-18
61	76.50	177.69 W	6-Jan-96	MAG-20
61	76.49	177.65 W	7-Jan-96	MAS-4D
73	76.38	177.41 W	9-Jan-96	MAS-4R
77	76.49	177.72 E	10-Jan-96	MAG-23
78	76.48	176.52 E	10-Jan-96	MAG-24
80	76.49	174.21 E	10-Jan-96	MAG-26
83	76.48	170.89 E	11-Jan-96	MAG-28
85	76.50	168.45 E	11-Jan-96	MAG-29
88	76.50	164.98 E	12-Jan-96	MAS-5D
88	76.49	164.83 E	12-Jan-96	MAG-31
89	76.49	163.83 E	12-Jan-96	MAG-32
90	75.99	165.00 E	13-Jan-96	MAG-33
92	76.46	164.77 E	13-Jan-96	MAG-35
93	76.75	164.98 E	13-Jan-96	MAG-36
94	77.00	164.98 E	14-Jan-96	MAG-37
95	76.43	164.58 E	14-Jan-96	MAS-5R

The means of collection was by either a remotely operated vehicle (ROV), or a MAGENUM (MAG) cast. Flux/sinking speed determinations by the MASCOT (MAS) system are also listed.

diameter, perimeter, aspect ratio, area, and other features, but all lengths reported here are the width of the aggregates normal to their vertical axis.

2.2. Aggregate sinking rates

Determinations of aggregate export rates requires the measurement of either in situ sinking speeds or fluxes of the particles, and the MASCOT (Marine Aggregate Settling Collector and Observation Tube) has the capability to measure both (Diercks and Asper, 1997). This instrument consists of a clear settling chamber that is viewed from the side and from below by a pair of cameras. The cameras are the same as used on the MAGENUM except that they have Zeiss wide-angle lenses installed to permit a more compact unit with minimal image distortion. Images from each of these cameras were subtracted from consecutive images to remove the background and leave in the image only the newly arrived aggregates or those that had moved. These subtracted images were then examined and analyzed for sinking speed (distance traveled on images from the horizontal camera) or flux (amount of newly arrived material on images from the vertical camera) per unit time. To estimate the total amount of material contained in aggregates, the raw data were converted into an estimated volume by estimating its effective radius from the area occupied on the image and assuming that each aggregate was a sphere. The images from the horizontal camera include the bottom surface of the viewing chamber, but because of the oblique nature of the configuration, the estimated fluxes should be considered only as coarse estimates.

The system was suspended at 175 m on a drifting sediment trap array that was designed to insulate it from wave-induced motion to the maximum extent possible (Asper and Smith, 1999). In order to assess the stability and performance of the array, a Woods Hole Instrument Systems electromagnetic current meter was attached at 175 m, and 5–10 Brancker thermographs, which record temperature to 0.1 °C and depth to 0.1 m, were attached along the wire. This information was used to examine the tilt or movement of the array, which is particularly important if the entire array is transported significantly by wind or ice.

The cameras were programmed to acquire images at intervals that we expected would yield quantifiable results given the anticipated aggregate

sinking rates. The upward-looking camera, which measures flux, was programmed to acquire an image every 4 min. In order to enhance the system's ability to measure a wide range of sinking speeds, the horizontal-looking camera was programmed to expose each film frame 4 times at 1-min intervals. Given the vertical dimension of the settling/observation chamber (20 cm), this plan would have produced at least two images of all aggregates settling less than 200 m d^{-1}, sinking rates consistent with those found in other oceanic realms (Honjo et al., 1984; Asper, 1987; Diercks and Asper, 1997).

3. Results

Ice concentrations during austral spring changed rapidly. Initially the entire region was covered by ice, although the ice in the region of the polynya was much thinner (<30 cm) than surrounding areas with little or no snow cover. By the end of the cruise, however, a substantial area of open water was observed. Ice remained along the coast in the west, as well as to the east near the shelf break. During late spring-early summer ice concentrations were further reduced. An ice barrier north of Ross Island separated the Ross Sea polynya from a coastal opening in the western Ross Sea, and ice continued to disappear to the north.

3.1. Vertical distributions of aggregate abundance and size

In nearly all cases aggregates were more abundant in the surface layer, with numbers declining at mid-depths (Fig. 2a and b). In general, there were low numbers of aggregates in spring, with abundance averaging 28.8, 17.4, 12.2 and 8.57 l^{-1} at 25, 50, 75 and 100 m (Table 2). Aggregate abundance increased in summer to more than twice what was observed in spring (Table 3), and the maximum abundance was found at 75 m at Station 88 (230 l^{-1}). Aggregate abundance at mid-depths was not markedly different between spring and summer (6.2 at 200 m in spring vs. 8.7 aggregates l^{-1} at 300 m in summer; Fig. 3), and the substantial seasonal increase was largely confined to the upper 150 m.

Abundance also varied dramatically in space and time. For example, at Station 49 during spring (11/28/94), the number of aggregates was less than 45 l^{-1} in the upper 100 m, and decreased to fewer than 10 l^{-1} below 100 m (Fig. 3a). During summer, Station 10 (12/23/95) had maximum aggregate concentrations of >60 l^{-1} near the surface, and the abundance again decreased to less than 10 l^{-1} at 200 m. Aggregate abundance at Station 85 ranged from 42 to 78 l^{-1} in the upper 100 m. This pattern paralleled that of POC (Fig. 3c), suggesting that small particles are affected by the same processes as aggregates. Unusual patterns of aggregate distribution also were noted at some sites, such as Station 21 in summer (12/27/95), where there were virtually no aggregates (<1 l^{-1}) near the surface (Fig. 3a), despite the fact that POC concentrations were substantial (Fig. 3c).

The sizes of aggregates, as determined by our photographic system, changed little with depth or time during the experiment, but the changes observed may be interesting and will be reported and discussed here. For example, the average size of an aggregate at Station 49 during spring was 1.1 mm in the upper 100 m, but increased at depth to slightly more than 1.2 mm (Fig. 3b). Similarly, the mean aggregate sizes for Stations 10 and 21 in summer were 1.0 and 1.1 mm, respectively, whereas the mean size of aggregates at Station 85 exceeded 1.4 mm (Fig. 3b). Aggregate sizes at depths ⩾100 m at Stations 10 and 21 increased slightly (Fig. 3b), but a larger increase was observed below 125 m at Station 38, where the mean size increased to 1.6 mm (more than double that observed at 50 m).

POC concentrations were elevated in the surface layer in both spring (1994) and summer (1995–1996), with relatively little difference in the mean POC concentration between the two seasons in the upper 50 m (Fig. 2c). Below that depth, however, POC concentrations in summer were significantly greater than during spring, suggesting that, if the years are comparable, a portion of the seasonal production pulse had been transferred to depth via slowly sinking particles or, alternatively, through the breakup of rapidly settling aggregates. POC

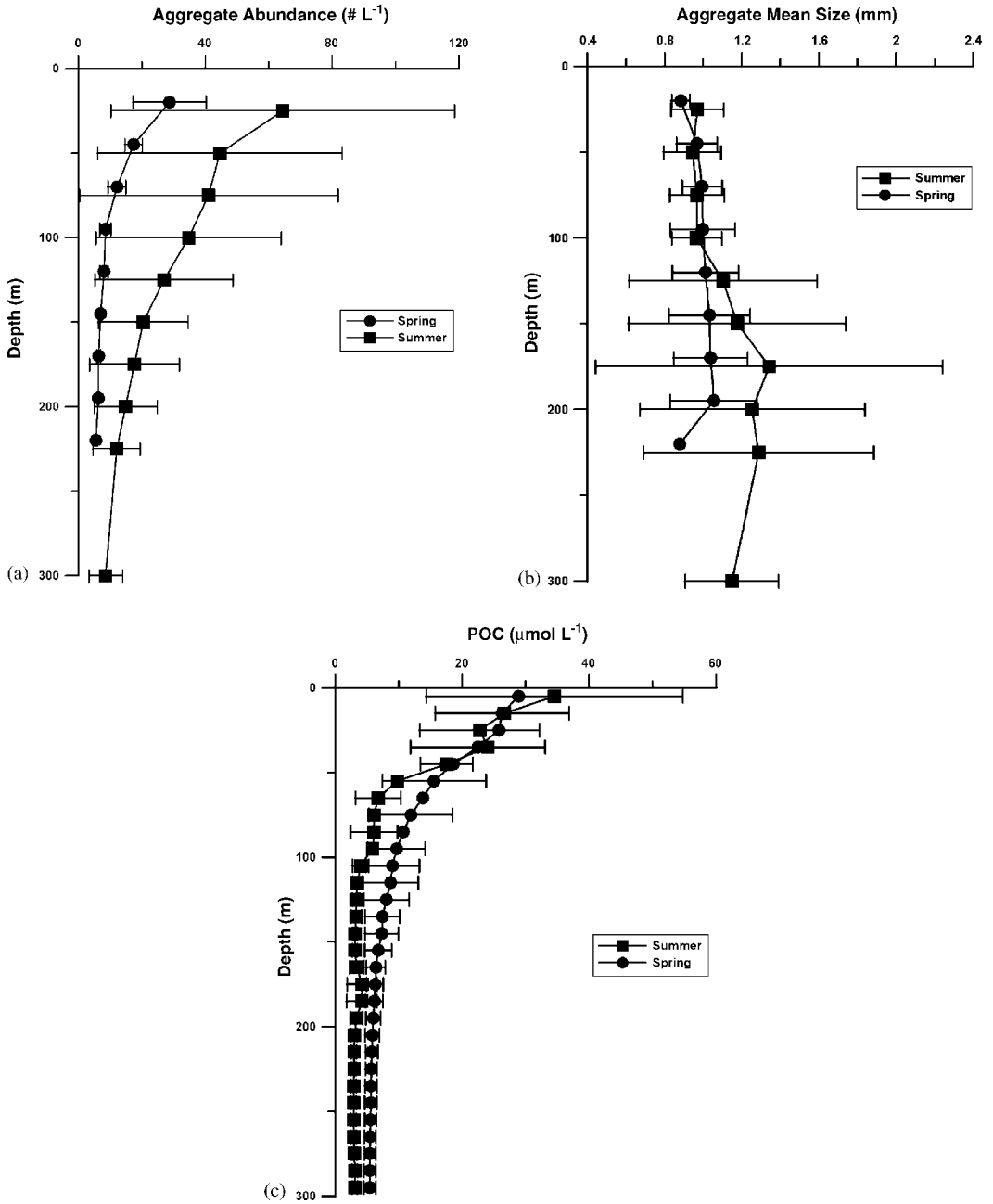

Fig. 2. Vertical profiles in the austral spring 1994 (●) and summer 1995–1996 (■) (a) average aggregate abundance (# l^{-1}) determined from camera profiles, (b) the mean size of aggregates (particles > 500 μm) from camera profiles (mm), and (c) the concentration of particulate organic carbon (μmol l^{-1}) from transmissometry. Transmissometry data converted to POC concentrations using a linear regression between beam attenuation and SPM (acquired simultaneously) and then from SPM to POC assuming a constant SPM/POC ratio. Plotted values of POC represent binned averages from 10-m intervals; aggregate values represent 25-m intervals. Standard deviations indicated by the error bars. Spring depths offset upward by 5 m for clarity in (b), whereas error bars for only every other depth in (c) are shown.

Table 2
Vertical distribution of aggregate abundance (mean, minimum and maximum) and particulate organic carbon (POC) concentration at that depth during austral spring, 1994

Dates	Depth (m)	Mean aggregate abundance (l^{-1})	Minimum abundance (l^{-1})	Maximum abundance (l^{-1})	n	Mean euphotic zone depth (m)	Mean mixed layer depth (m)	(POC) ($\mu mol\,l^{-1}$)
11/28–29/94	25	36.6	28.0	45.2	2	33	37	8.81
	50	18.9	17.0	20.7	2			6.09
	75	14.1	11.9	16.2	2			2.55
	100	9.6	9.4	9.8	2			2.90
	150	7.0	6.7	7.4	2			3.08
	200	6.2	6.1	6.3	2			2.63
12/1–2/94	25	20.9	20.4	21.4	2	32	40	25.7
	50	15.9	14.1	17.8	2			7.05
	75	10.4	9.5	11.2	2			4.46
	100	3.3	—	6.5	1			2.48
	150							2.21
	200							1.99

Aggregate statistics represent the summation of data collected from 5 m above and below the listed depth.

profiles at individual stations also illustrated the variations in space and time (Fig. 3c). Spring POC concentrations (Station 49) were less than those observed in summer, and the stations within the summer cruise generally showed an increase with time (most data not shown), although a decrease at the surface from the seasonal maximum was noted by mid-January (Station 85). POC levels within these four stations were higher at the surface than at depth, with a maximum value at Station 21 ($53.2\,\mu mol\,l^{-1}$). The latter two stations in summer (Stations 21 and 85) had quantitatively similar profiles below 65 m, but Station 85 had substantially reduced POC levels above that. Although the stations were in different locations, the pattern suggests that the seasonal reduction in POC in the surface layer may have resulted from the production of large, rapidly sinking aggregates that disappeared from the upper 200 m of the water column.

3.2. Horizontal distributions of aggregate abundance and size

The 76°30′S transect is characterized by significant spatial variability with regard to hydrography, nutrient concentrations, and phytoplankton biomass and assemblage composition (Smith et al., 1996; Smith and Asper, 2001), and we also expected substantial variations in aggregate abundance. In summer, ice concentrations had decreased substantially, and within the eastern portion of the transect where little ice was present, aggregates were abundant during our first occupation (Fig. 4a). In the center of the transect, the number of aggregates increased further, but north of Ross Island (an area that was ice covered), the water was extremely clear with few aggregates (Fig. 4a and b). At the extreme western portion of the transect in open water, we observed aggregate abundance to be maximal ($>100\,l^{-1}$; Station 25; Fig. 4a).

The spatial distribution of aggregate size appeared to be roughly opposite that of abundance (Fig. 4b), but this relationship could not be shown to be statistically significant (t test, $P = 0.05$). Maximum sizes were found in the region of minimum abundance; conversely, minimum sizes occurred in both the extreme west and east and corresponded with elevated abundance of aggregates. A similar size/abundance relationship was observed near Station 85 (Fig. 3a and b). Aggregate abundance and POC concentration distributions appeared to be similar to each other, with

Table 3
Vertical distribution of aggregate abundance (mean ± standard deviation, minimum and maximum, number (n) of profiles), mean euphotic zone depth, mean mixed layer depth, and particulate organic carbon (POC) concentration during austral summer, 1995–1996

Dates	Depth (m)	Mean aggregate abundance (l^{-1})	Minimum abundance (l^{-1})	Maximum abundance (l^{-1})	n	Mean euphotic zone depth (m)	Mean mixed layer depth (m)	POC ($\mu mol\,l^{-1}$)
12/22–29/95	25	51.9 ± 50.7	0.288	125.6	7	20.8	22.6	36.3
	50	48.5 ± 32.9	0.423	104.5	9			20.4
	75	36.2 ± 33.5	0.429	107.4	9			9.65
	100	23.3 ± 19.2	0.336	56.3	9			9.32
	150	122 ± 304	0.279	982.7	9			5.55
	200	8.9 ± 7.8	0.475	24.0	7			ND
	300	8.0 ± 8.9	0.266	29.1	7			ND
12/30/95–1/3/96	25	19.2 ± 43.0	0	115.5	6	27.2	14.6	24.5
	50	65.8 ± 23.3	34.2	103.0	6			24.4
	75	64.0 ± 21.5	29.1	92.6	6			16.4
	100	60.3 ± 10.7	42.7	74.4	6			9.91
	150	24.9 ± 9.5	6.9	36.9	6			5.23
	200	15.4 ± 5.9	7.8	22.7	6			ND
	300	8.4 ± 3.9	5.1	15.5	6			ND
1/6–12/96	25	ND	ND	ND		32.9	28.0	19.7
	50	42.0 ± 68.7	0	200.4	3			13.0
	75	51.1 ± 76.4	0	230.5	4			8.64
	100	50.1 ± 48.7	0	159.0	6			7.38
	150	31.3 ± 20.9	12.6	73.4	7			5.54
	200	17.5 ± 10.4	10.0	41.2	7			2.54
	300	7.9 ± 3.1	5.8	15.2	7			1.35
1/13–14/96	25	77.6 ± 77.7	0.0	206.5	3	29.7	8.83	24.3
	50	59.8 ± 33.8	35.1	118.0	4			7.54
	75	60.0 ± 35.6	29.2	120.3	4			10.3
	100	54.6 ± 29.6	25.1	101.8	4			6.76
	150	24.1 ± 9.4	9.7	35.6	4			6.20
	200	19.3 ± 11.8	7.0	38.7	4			5.27
	300	6.3 ± 1.1	4.7	7.6	4			ND

Aggregate statistics represent the summation of data collected from 5 m above and below the listed depth. ND = no data.

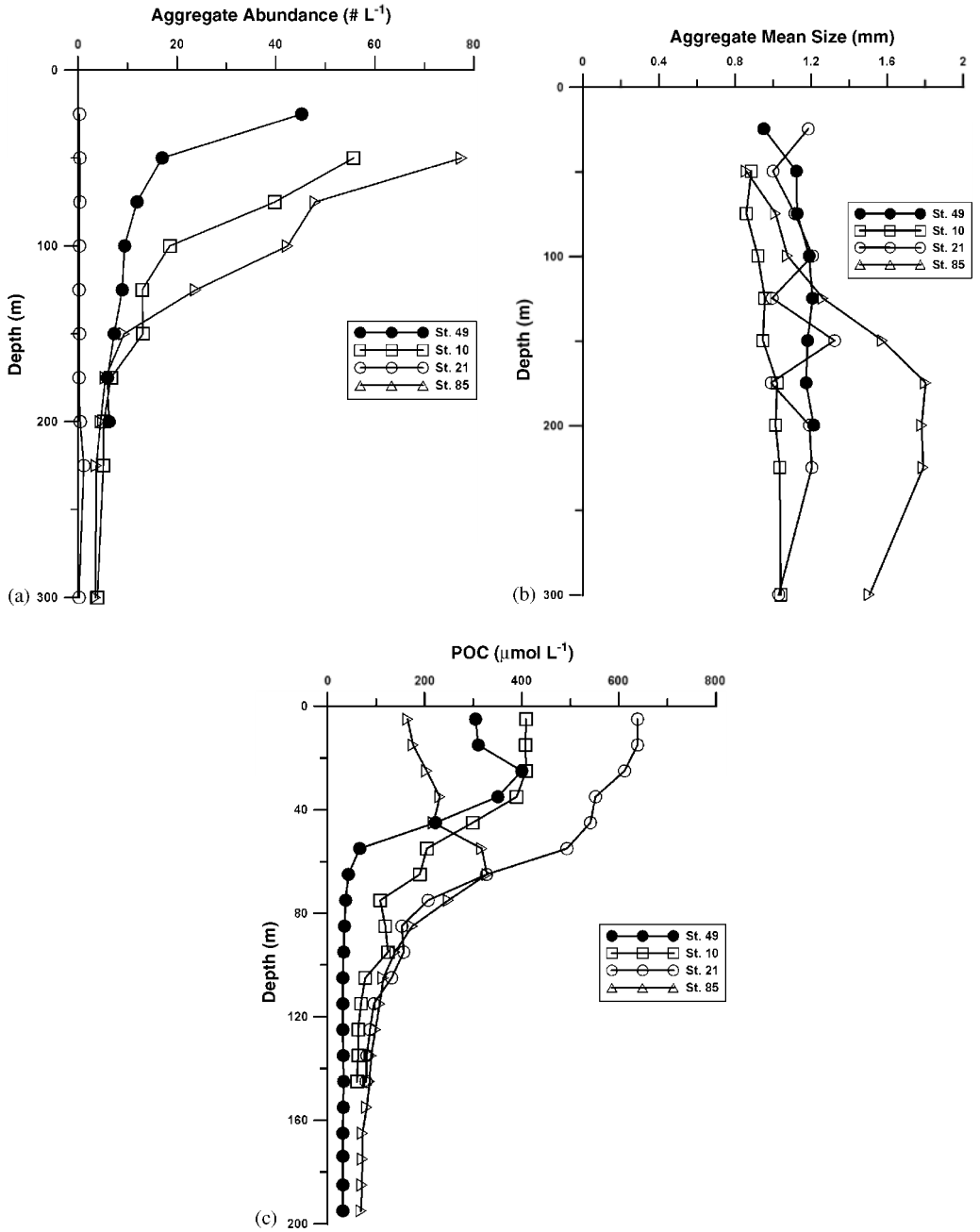

Fig. 3. Vertical distributions of (a) aggregate abundance (# l^{-1}), (b) aggregate mean size (mm), and (c) concentration of particulate organic carbon at Station 49 (11/28/94), Station 10 (12/23/95), Station 21 (12/27/95) and Station 85 (1/11/96). Binning as described in Fig. 2.

elevated POC levels occurring in the surface and spatially correlated with higher aggregate abundance (Fig. 4a and c). However, some locations did appear to deviate from this relationship (e.g., Station 19, Fig. 4), with elevated aggregate abundance but moderate POC levels. Station 21

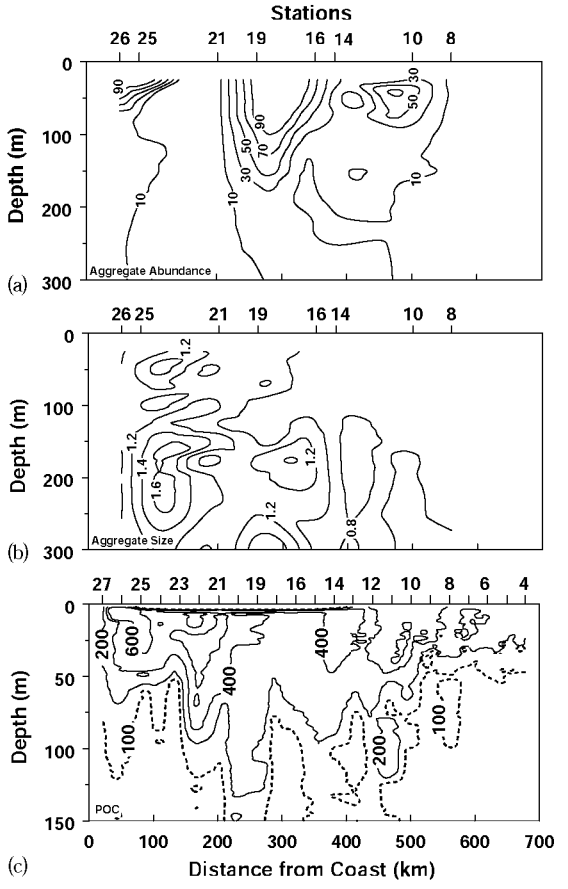

Fig. 4. Vertical sections of (a) aggregate abundance (# l^{-1}), (b) aggregate size (mm), and (c) particulate organic carbon concentration (μmol l^{-1}) along 76°30′S during December 22–29, 1995.

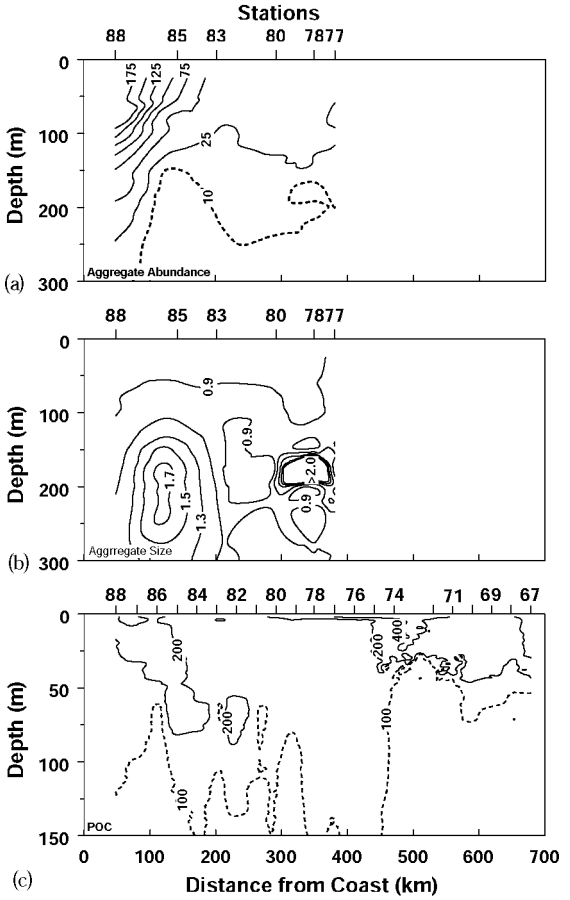

Fig. 5. Vertical sections of (a) aggregate abundance (# l^{-1}), (b) aggregate mean size (mm), and (c) particulate organic carbon concentration (μmol l^{-1}) along 76°30′S during January 8–14, 1996.

(Fig. 3) was highly unusual: it showed high POC concentrations but aggregates were nearly non-existent.

During an occupation of the same transect in mid-summer, aggregate abundance and particle concentrations changed markedly (Fig. 5a–c). Maximum aggregate abundance was found in the western portion of the transect, whereas aggregate concentrations were nearly an order of magnitude lower in the south central and eastern portion. Sizes decreased in the west (Station 88), where abundance was greatest, and sizes were maximal (Station 79) at depth, where abundance was low (Fig. 5a and b). POC and aggregate abundances again appeared to be spatially correlated (Fig. 5a and c).

3.3. Temporal changes

To assess temporal changes in aggregates, particle concentrations along 76°30′S were determined twice in 1996. Mean aggregate abundances along the transect were calculated by averaging data from the same depths at all stations. In the surface layer, aggregate abundance was approximately two-fold greater in January than in December at the surface but was similar at depths below 300 m (Fig. 6a). Aggregate size was slightly

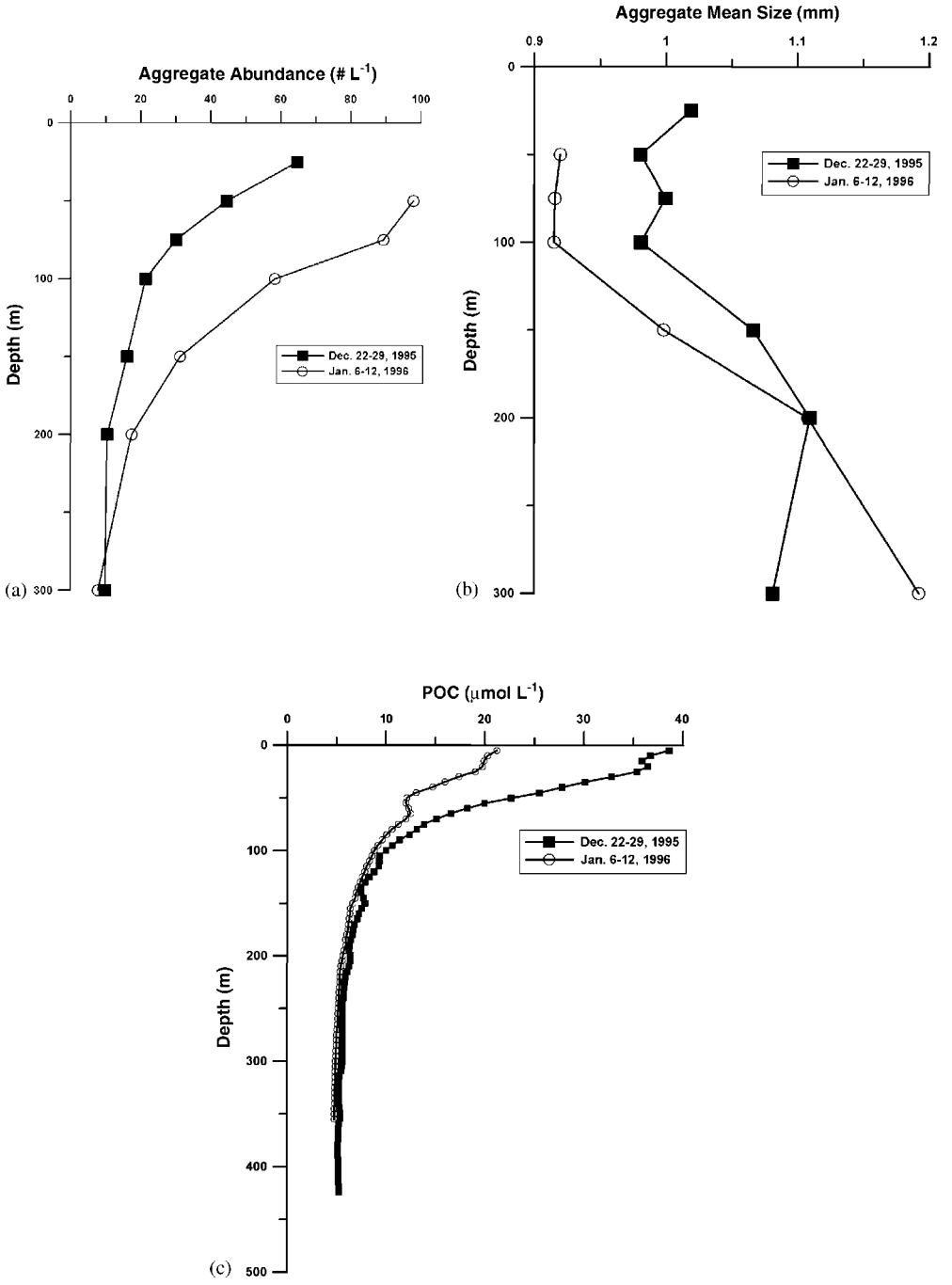

Fig. 6. Variations in average (a) aggregate abundance (# l^{-1}), (b) aggregate mean size (mm), and (c) particulate organic carbon concentration (μmoll^{-1}) between occupations of the transects in December 22–29, 1995 and January 6–12, 1996.

greater during the first transect, particularly at the surface (Fig. 6b). POC concentrations decreased in the surface layer (Fig. 6c). Individual stations also illustrate this trend. For example, at Station 10 (12/23/95) POC concentrations at the surface were 34.1 μmol l^{-1}, but had decreased to 27.8 μmol l^{-1} by January 9, 1996 (Figs. 3c and 4b).

3.4. Effect of phytoplankton assemblage composition

Because the region often has distinct phytoplankton assemblages which are characterized by different dominant taxa (DiTullio and Smith, 1996; Arrigo et al., 1999; Smith and Asper, 2001), it is possible to contrast these locations to test if phytoplankton assemblage regulates aggregate abundance, particle concentration, and aggregate size. Dominance of taxa was determined according to the ratio of the xanthophyll accessory pigments fucoxanthin (a diatom pigment) and 19′-hexanoyloxyfucaxanthin (characteristic of *Phaeocystis antarctica*) found in the water column (Smith and Asper, 2001). Two station pairs were examined: Station 14 and 73 (ca. 76°30′S, 177°36′E), which was dominated by *P. antarctica*, and Station 26 and 88 (ca. 76°30′S, 164°50′E), which was dominated by diatoms. Both pairs of stations were sampled approximately 15 days apart (14 and 17 days, respectively). Aggregate abundance was lower at Station 73 (dominated by *P. antarctica*) than at 88 (dominated by diatoms; i.e., 200 and 230 l^{-1} vs. 188 and 68 l^{-1} at 50 and 75 m; Fig. 7a), and early summer abundance is 3.3-fold larger in diatom-dominated regions in the upper 50 m (Fig. 7a). Mean size distributions of aggregates in diatom-dominated regions overlapped those from *P. antarctica*-dominated stations, as did POC concentrations (Fig. 7b). Therefore, the only difference we noted in regions with markedly different taxonomic character was in aggregate abundance in surface waters.

3.5. Sinking speeds and fluxes

Equipment malfunctions (including leaks, film breakage and shutter failures) prevented the vertical camera from acquiring useful data, but the horizontal camera performed well. Images from this camera were used to determine sinking speeds, but they also included the floor of the chamber so coarse estimates of aggregate flux could be obtained from these oblique views. Sinking speeds of the aggregates in successive photographs from this camera ranged from near zero to more than 200 m d^{-1}. However, many more aggregates arrived on the bottom surface of the imaging chamber than were seen in transit. At Station 36 (MAS-3), for example, most images contained from 2 to 12 aggregates that had settled during the 4 min exposure interval, resulting in a calculated flux of $4–24 \times 10^3$ aggregates m^{-2} h^{-1}. In contrast, these same images contained on average less than one aggregate in transit, suggesting that >90% of the aggregates actually arriving on the bottom of the chamber settled too quickly to be detected in successive images. Therefore, the minimum sinking rates of these aggregates were in excess of 288 m d^{-1}.

4. Discussion

The southern Ross Sea represents an extraordinary location to observe the dynamics of aggregates because it is well known for its blooms of both of *Phaeocystis antarctica* and diatoms (DiTullio and Smith, 1996; Arrigo et al., 1999), and the temporal patterns of these blooms are relatively well known (Smith et al., 2000; Gardner et al., 2000; Sweeney et al., 2000). A transect across the region is analogous to sampling in time, since stations recently exposed to light by removal of the ice (in the north and on the edges of the polynya) represent early stages of growth (Arrigo et al., 1998). In contrast, stations in the south central Ross Sea have been ice free for longer (Smith et al., 2000), and the plankton there have likely had a much different growth pattern than those that have only recently been exposed to full solar irradiance. Given the range of phytoplankton biomass, environmental conditions, and assemblage composition, a wide range of aggregate abundance and dynamics would be expected.

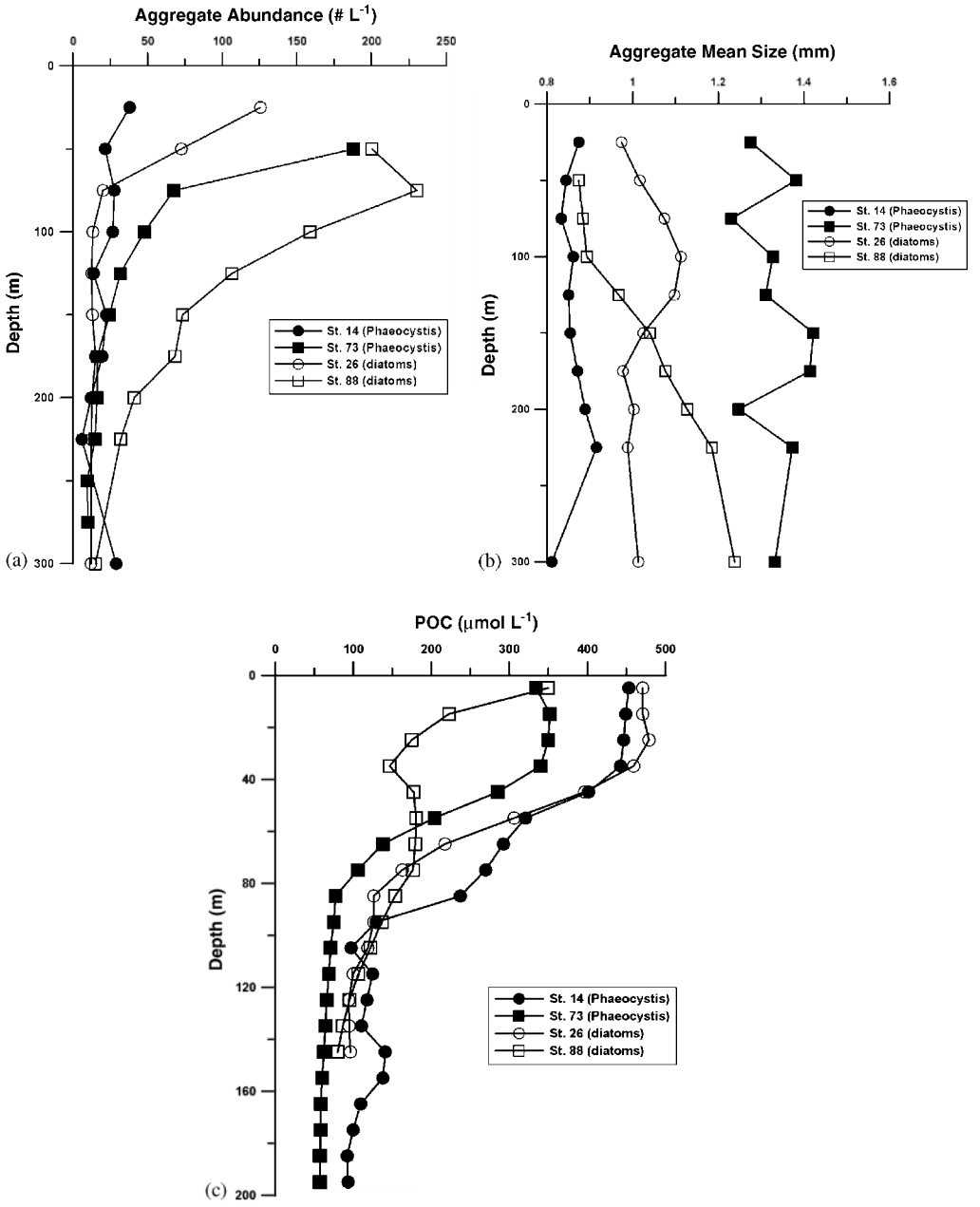

Fig. 7. (a) Aggregate abundance (# l^{-1}), (b) mean size (mm), and (c) particulate organic carbon concentrations (µmol l^{-1}) at stations dominated by diatoms (Station 26 and 88) and *Phaeocystis antarctica* (Station 14 and 73).

The abundance of aggregates we found in the Ross Sea (maximum of 230 l^{-1}) is among the highest reported to date for natural conditions (Table 4). Oligotrophic systems generally have an abundance of 10 l^{-1} or less, but the trophic state of a region is a weak predictor of the number and importance of aggregates. Aggregate abundance is a complex function of both production and losses, with environmental factors such as coagulation enhancers like TEP (Hong et al., 1997), particle

Table 4
Compendium of aggregate abundance estimates from various oceanic regions

Study site	Maximum aggregate abundance (l^{-1})	References
Southern California bight	1.1	Alldredge and Cox (1982)
Diatom mesocosm	6000	Alldredge et al. (1995)
Panama basin	2.4; 4–6	Asper (1987), Asper et al. (1992a,b)
Southern California bight	7.6	Beers et al. (1986)
Ems and Rhine estuaries	968	Eisma, 1986
Louisiana shelf	60	Gardner and Walsh (1990)
Gulf of Mexico	3	Gardner and Walsh (1990)
Mediterranean	20	Gorsky et al. (1992)
Mediterranean	80	Gorsky et al. (2000)
California coast	79	Graham et al. (2000)
Monterey Bay	7	Honjo et al. (1984)
St. Helena Bay, South Africa	640	Kiørboe et al. (1998)
Northeast Atlantic	12	Lampitt et al. (1993)
California coast	60	McIntyre et al. (1998)
Monterey Bay, CA: upwelling	40	Pilskaln et al. (1998)
Monterey Bay, CA: non-upwelling	5	Pilskaln et al. (1998)
North Sea	400	Riebesell (1991)
Gullmar fjord, Sweden	32	Tiselius and Kuylenstierna (1996)
Monterey Bay	28	Trent et al. (1978)
Ross Sea, Antarctica	230	This study

stickiness, turbulence, and collision frequency being important in controlling coagulation, and zooplankton grazing and bacterial oxidation being important in regulating loss rates. Indeed, it has been proposed that a "critical concentration" of aggregates exists. This concentration represents a balance between production from smaller particles and sedimentation losses induced by increased sinking rates of larger aggregates (Jackson, 1990; Kiørboe et al., 1994).

The role of aggregates in export from the surface layer can be investigated in at least three ways: (1) by examining the material collected in sediment traps, quantifying fecal material and estimating the contribution of aggregates as the difference between total flux and fecal pellet flux, (2) by measuring the in situ flux directly, and (3) by quantifying the loss of aggregates from the surface layer and observing their appearance in deeper layers. Asper and Smith (1999) measured export from the mixed layer using floating sediment traps and found that aggregates appeared to be very important in the export process. Conversely, they found a minimal contribution of zooplankton grazing and fecal pellet flux to losses from the surface layer. Similarly, Dunbar et al. (1998) found that in the central Ross Sea loosely defined aggregates were a major portion of the organic flux to depth (250 and 550 m). Smith and Dunbar (1998) investigated the relationship between new production and vertical flux, and found that a substantial (ca. 2 month) temporal offset occurs in the south central Ross Sea (that region dominated by *P. antarctica*) between maximum rates of new production and maximum fluxes to 250 m. They suggested that this weak coupling (temporal lag) was due to the low sinking rates of small particles, the temporal offset between production and large aggregate formation, and the export of these large aggregates to depth. Our results are consistent with this suggestion.

Although direct measurements of flux provide the most compelling results, the data presented here are unfortunately limited. These results show that aggregates settle at a wide variety of speeds, with some of the aggregates appearing to settle at speeds of at least 288 m d^{-1} under the low turbulence conditions generated within our observation chamber. These sinking rates probably

represent an extreme end of the settling speed spectrum but are qualitatively consistent with other flux determinations, including the floating sediment trap data (Asper and Smith, 1999). The MASCOT system also represents an unusual configuration for a sediment trap because of its cylindrical vertical tubes emptying into a rectangular chamber. This could help to explain why it collected material at a slightly higher rate than the VERTEX-type sediment traps (Table 5), but the difference between them appears to be within the range of error often associated with sediment traps (Gardner, 2000). The coarse estimates of the flux of aggregates from the horizontal camera were correlated with mass flux (Table 5), supporting their role in vertical mass transport. Visual examination of the contents of the traps confirmed that the sample was dominated by flocculent material, with a relatively small contribution by fecal pellets.

The third method of evaluating aggregate flux is to examine the changes in abundance with time or depth in the water column. This method assumes no advective effects, which is reasonable based on the low advection rates indicated by the slow northward drift of our arrays (Asper and Smith, 1999). The difficulty with this approach, however, is that aggregates, once formed, can sink at extraordinarily high speeds and thus will rapidly disappear from the water column. It would therefore be expected that the slower an aggregate's sinking speed (and presumably the smaller its size), the more abundant it would be, and conversely, the higher its sinking speed, the less abundant it would be. This relationship was suggested by early modeling efforts (Jackson, 1990) and observations in a Danish fjord (Kiørboe et al., 1994). Our observations also support this relationship, as evidenced by the measured sinking speeds and by the data from the re-occupied stations. Station 61, 77, 78 and 83, for example, represent re-occupations of Station 10, 14, 16, and 21, respectively (Figs. 5 and 6). In all cases (except Station 83), aggregate abundance near the surface is the same as or lower than previously measured, but particle concentrations are dramatically lower than observed during the first occupation (often $<50\%$ of the initial concentration). Thus it appears that

Table 5
Vertical flux estimates from floating sediment trap and MASCOT deployments

Station number	Location	Sediment trap mass flux ($mg\,m^{-2}\,d^{-1}$)	Sediment trap carbon flux ($mg\,m^{-2}\,d^{-1}$)	MASCOT mass flux ($mg\,m^{-2}\,d^{-1}$)	MASCOT carbon flux ($mg\,m^{-2}\,d^{-1}$)	Aggregate flux ($m^{-2}\,h^{-1}$)	Aggregate flux ($mm^3\,m^{-2}\,h^{-1}$)	Average aggregate size (mm)	Mass per aggregate volume
14	171.8°E	263	78	369	109	ND	ND	ND	ND
21	170.8°E	521	114	819	183	1300	500	2.1	1.6
40	165.0°E	1404	162	2038	231	12,500	24,700	2.2	0.08
61	177.6°W	852	106	979	131	ND	ND	ND	ND
94	165.0°E	1135	121	1544	165	6300	4000	2.1	0.386

Complete description of sediment trap data in Asper and Smith (1999). All stations occupied on the 76°30′S transect. ND = no data.

aggregates are continually being formed by the coagulation of smaller particles and exported. This simultaneous addition through aggregation and removal by settling results in an aggregate abundance that is the result of the balance between formation and export. This balance will change continuously throughout the season as the general controls over these processes change. During our study in the Ross Sea, this balance resulted in relatively high concentrations, but the specific reasons and control functions remain unclear and would require a study that is entirely focused on this phenomenon.

Many of these aggregates may reach the sea floor (given the rapid sinking rates we observed) within ca. 2–3 days. However, a large fraction is thought to dis-aggregate below the mixed layer and contribute to the abundance of fine particles at depth. This relationship is supported by the reduced mass flux observed in floating sediment traps at 200 m relative to that at 100 m (Asper and Smith, 1999), and is also suggested by the increased concentration of suspended particulate matter below the mixed layer (Figs. 6 and 7). This process may also be responsible for the increased abundance of suspended particulate material in the bottom nepheloid layer (Ditullio et al., 2000).

In contrast to the south central Ross Sea, the region near 76°30′S, 165°E is often dominated by diatom assemblages. The highest concentrations of aggregates in the entire study were observed in this area, with aggregate abundance at Station 93 exceeding 230 l^{-1}. It appeared that there were relatively more aggregates in diatom-dominated areas than in *P. antarctica*-dominated ones (Fig. 7a and b) This observation should not, however, be interpreted as an indication that *P. antarctica* forms fewer aggregates than diatom assemblages. On the contrary, it is possible that a similar number of aggregates are formed by *P. antarctica*, but that these aggregates are exported soon after formation, leaving fewer aggregates remaining in the water column. Given the flux estimates described above and the overall loss of biomass detected, it is therefore possible that the aggregates formed by *P. antarctica*, in this region and during this season, settle faster than diatom aggregates and therefore are removed from the surface layer more rapidly.

Assessments of stickiness of a variety of diatoms and of *Phaeocystis* sp. have been made in controlled laboratory settings (Kiørboe et al., 1990; Kiørboe and Hansen, 1993; Passow and Wassmann, 1994; Hansen et al., 1996). These laboratory results suggest that *Phaeocystis* does not have a greater potential to form aggregates, and in fact may have less than some diatoms. Our data cannot be used to directly address this question, because of the non-linear relationship between aggregate genesis and losses, as well as the different temporal growth patterns of the two assemblages. Our data did, however, show differences between the regions, including differences between the two diatom and the two *Phaeocystis* dominated sites (Fig. 7a and b), but we cannot conclusively demonstrate what factors are important in producing this difference.

Gardner et al. (2000) assessed the temporal variations in particulate organic matter concentrations in the southern Ross Sea and made estimates of export based on these changes. They also compared the loss rates to the accumulation rates found in moored sediment traps. The temporal patterns of losses and trap accumulation rates were noticeably different, as were the quantities of material that were found in the traps. Although a clear resolution of these discrepancies was not provided, Gardner et al. (2000) suggested that greater numbers of aggregates (detected optically using a SeaTech Light Scattering Sensor, which detects the reflection of light off individual particles in a greater volume of water than assessed by a transmissometer) were found in late summer-autumn, and that these may represent slowly sinking material that did not settle to the depth of the moored sediment traps until later in the season, facilitated by pteropod feeding. They found fewer aggregates in early spring and summer, a finding that is consistent with our results. Furthermore, their suggestion that aggregates were a major component of flux is also verified by our results (Table 5). A quantitative comparison among flux estimates made from camera systems, those derived from floating sediment traps (Asper and Smith, 1999) and those

measured by moored sediment traps (Dunbar et al., 1998) remains unavailable.

DiTullio et al. (2000) found substantial amounts of DMSP and chlorophyll *a* in the sediments, and these distributions correlated spatially with calculated export from the surface layer. Elevated concentrations of chlorophyll *a* and DMS were also found in a nepheloid layer near the bottom (550 m), and it was suggested (based on a fluorometric determination of phytoplankton activity) that the material found at the sediment surface and in the nepheloid layer was only recently delivered to depth. Their study was conducted from 18 December–8 January, 1996–1997and hence was similar to the timing of our 1995/96 cruise. Our results would suggest that the sedimentary and bottom-layer particles they observed were generated in the surface layer, coagulated to form large aggregates, and traversed the water column rapidly (in a few days), thereby retaining many of their surface properties.

In conclusion, our data suggest that in the Ross Sea aggregate formation and flux are critical components of the particulate carbon dynamics. Aggregate formation and flux are the largest loss term to the particulate load in surface waters and they exert a strongly structuring force in regulating phytoplankton assemblage biomass. Aggregates increased seasonally in abundance, and concentrations found in the Ross Sea are greater than most other places in the ocean assessed to date. At least some aggregates appear to sink very rapidly ($>288\,m\,d^{-1}$) and represent a mechanism by which material from the surface layer can reach the benthos rapidly. Despite their importance, our knowledge of the dynamics of aggregates remains incomplete, and further assessments of the environmental and biological controls on their production and destruction are necessary to quantitatively understand their role in oceanic carbon cycles.

Acknowledgements

This research was supported by NSF Grants OPP-9317598 to VLA and OPP-9317587 to WOS. We thank M. Tuel, S. Polk, J. Seward, L.W. Smith and A.-M. White for technical assistance, and Dr. Keith Moore (NCAR) for help with the ice distribution analyses. We are indebted to the two anonymous reviewers who provided comments and W. Gardner who provided detailed and insightful suggestions which substantially improved this manuscript. This paper is dedicated to the memory of Joon Jae Lee, who performed many of the analyses for this project, but whose accidental death prevented his involvement in its completion.

References

Alldredge, A.L., 1998. The carbon, nitrogen and mass content of marine snow as a function of aggregate size. Deep-Sea Research I 45, 529–542.

Alldredge, A.L., Cox, J.L., 1982. Primary productivity and chemical composition of marine snow in surface waters of the Southern California Bight. Journal of Marine Research 40, 504–527.

Alldredge, A.L., Silver, M., 1988. Characteristics, dynamics and significance of marine snow. Progress in Oceanography 20, 41–82.

Alldredge, A.L., Gotschalk, C., Passow, U., Riebesell, U., 1995. Mass aggregation of diatom blooms: insights from a mesocosm study. Deep-Sea Research II 42, 9–27.

Arrigo, K.R., McClain, C.R., 1994. Spring phytoplankton production in the western Ross Sea. Science 266, 261–263.

Arrigo, K.R., Weiss, A.M., Smith Jr., W.O., 1998. Physical forcing of phytoplankton dynamics in the western Ross Sea. Journal of Geophysical Research 103, 1007–1022.

Arrigo, K.R., Robinson, D.H., Worthen, D.L., Dunbar, R.B., DiTullio, G.R., Van Woert, M., Lizotte, M.P., 1999. Phytoplankton community structure and the drawdown of nutrients and CO_2 in the Southern Ocean. Science 283, 365–367.

Asper, V.L., 1987. Measuring the flux and sinking speed of marine snow aggregates. Deep-Sea Research 34, 1–17.

Asper, V.L., Smith Jr., W.O., 1999. Particle fluxes during austral spring and summer in the southern Ross Sea (Antarctica). Journal of Geophysical Research 104, 5345–5359.

Asper, V.L., Deuser, W.G., Knauer, G.A., Lohrenz, S.E., 1992a. Rapid coupling of sinking particle fluxes between surface and deep ocean waters. Nature 357, 670–672.

Asper, V.L., Honjo, S., Orsi, T.H., 1992b. Distribution and transport of marine snow aggregates in the Panama Basin. Deep-Sea Research 39, 939–952.

Beers, J.R., Trent, J.D., Reid, F.M.H., Shanks, A.L., 1986. Macroaggregates and their phytoplanktonic components in the Southern California Bight. Journal of Plankton Research 8 (3), 475–487.

Caron, D.A., Dennett, M.R., Lonsdale, D.J., Moran, D.M., Shalapyonok, L., 2000. Microzooplankton herbivory in the Ross Sea, Antarctica. Deep-Sea Research II 47, 3249–3272.

Chung, S.P., Gardner, W.D., Richardson, M.J., Walsh, I.D., Landry, M.R., 1996. Beam attenuation and microorganisms: spatial and temporal variations in small particles along 140°W during 1992 JGOFS-EqPac transects. Deep-Sea Research II 43, 1205–1226.

Comiso, J.C., McClain, C.R., Sullivan, C.W., Ryan, J.P., Leonard, C.L., 1993. Coastal zone color scanner pigment concentrations in the southern ocean and relationships to geophysical surface features. Journal of Geophysical Research 98, 2419–2451.

Diercks, A.-R., Asper, V.L., 1997. In situ settling speeds of marine snow aggregates below the mixed layer: Black Sea and Gulf of Mexico. Deep-Sea Research I 44, 385–398.

DiTullio, G.R., Smith Jr., W.O., 1996. Relationship between dimethylsulfide and phytoplankton pigment concentrations in the Ross Sea, Antarctica. Deep-Sea Research I 42, 873–892.

DiTullio, G.R., Grebmeier, J.M., Arrigo, K.R., Lizotte, M.P., Robinson, D.H., Leventer, A., Barry, J.P., Van Woert, M.L., Dunbar, R.B., 2000. Rapid and early export of *Phaeocystis antarctica* blooms in the Ross Sea Antarctica. Nature 404, 595–598.

Dunbar, R.B., Leventer, A.R., Mucciarone, D.A., 1998. Water column sediment fluxes in the Ross Sea, Antarctica (I): atmospheric and sea ice forcing. Journal of Geophysical Research 102, 30741–30759.

Eisma, D., 1986. Flocculation and de-flocculation of suspended matter in estuaries. Netherlands Journal of Sea Research 20, 183–199.

Gardner, W.D., 2000. Sediment trap sampling in surface waters. In: Hanson, R.B., Ducklow, H.W., Field, J.G. (Eds.), The Changing Ocean Carbon Cycle. Cambridge University Press, Cambridge, pp. 240–281.

Gardner, W.D., Walsh, I.D., 1990. Distribution of macroaggregates and fine-grained particles across a continental margin and their potential role in fluxes. Deep-Sea Research I 37, 401–411.

Gardner, W.D., Richardson, M.J., Smith Jr., W.O., 2000. Seasonal build-up and loss of POC in the Ross Sea. Deep-Sea Research II 47, 3423–3450.

Gorsky, G., Picheral, M., Stemmann, L., 2000. Use of the underwater video profiler for the study of aggregate dynamics in the north Mediterranean. Estuarine and Coastal Shelf Science 50, 121–128.

Gorsky, G., Aldorf, C., Kage, M., Picheral, M., Garcia, Y., Favole, J., 1992. Vertical distribution of suspended aggregates determined by a new video profiler. Annuales de l'Institut Oceanographique 68, 1–7.

Gowing, M.M., Garrison, D.L., Kunze, H.B., Winchell, C.J., 2001. Biological components of Ross Sea short-term particle fluxes in the austral summer of 1995–1996. Deep-Sea Research I 48, 2645–2671.

Graham, W.M., MacIntyre, S., Alldredge, A.L., 2000. Diel variations of marine snow concentration in surface waters and implications for particle flux in the sea. Deep-Sea Research I 47, 367–395.

Hansen, J.L.S., Kioerboe, T., Alldredge, A.L., 1996. Marine snow derived from abandoned larvacean houses: sinking rates, particle content and mechanisms of aggregate formation. Marine Ecology Progress Series 141, 205–215.

Hong, Y., Smith, W.O., White, A.-M., 1997. Studies on transparent exopolymer particles (TEP) in the Ross Sea (Antarctica) and by *Phaeocystis Antarctica* (Prymnesiophyceae). Journal of Phycology 33, 368–376.

Honjo, S., Doherty, K.W., Agrawal, Y.C., Asper, V.L., 1984. Direct optical assessment of large amorphous aggregates (marine snow) in the deep ocean. Deep-Sea Research 31, 67–76.

Jackson, G.A., 1990. A model of the formation of marine algal flocs by physical coagulation processes. Deep-Sea Research 37, 1197–1211.

Jackson, G.A., 1995. Comparing observed changes in particle size spectra with those predicted using coagulation theory. Deep-Sea Research II 42, 159–184.

Jackson, G.A., Lochmann, S.E., 1992. Effect of coagulation on nutrient and light limitation of an algal bloom. Limnology and Oceanography 37, 77–89.

Jacobs, S.S., Comiso, J.C., 1991. Sea ice and oceanic processes on the Ross Sea continental shelf. Journal of Geophysical Research 94, 18195–18212.

Kiørboe, T., Hansen, J.L.S., 1993. Phytoplankton aggregate formation: observations of patterns and mechanisms of cell sticking and the significance of exopolymeric material. Journal of Plankton Research 9, 993–1018.

Kiørboe, T., Anderson, K.P., Dam, H.G., 1990. Coagulation efficiency and aggregate formation in marine phytoplankton. Marine Biology 107, 235–245.

Kiørboe, T., Lundsgaard, C., Olsen, M., Hansen, J.L.S., 1994. Aggregation and sedimentation processes during a spring phytoplankton bloom: a field experiment to test coagulation theory. Journal of Marine Research 52, 297–323.

Kiørboe, T., Tiselius, P., Mitchell-Innes, B., Hansen, J.L.S., Visser, A.W., Mari, X., 1998. Intensive aggregate formation with low vertical flux during an upwelling-induced diatom bloom. Limnology and Oceanography 43, 104–116.

Lampitt, R.S., Hillier, W.R., Challenor, P.G., 1993. Seasonal and diel variation in the open ocean concentration of marine snow aggregates. Nature 362, 737–739.

Markus, T., 1999. Results from an ECMWF-SSM/I forced mixed layer model of the Southern Ocean. Journal of Geophysical Research 104, 15603–15620.

Mathot, S., Smith Jr., W.D., Carlson, C.A., Garrison, D.L., Gowing, M.M., Vichers, C.L., 2000. Carbon partitioning within *Phaeocytis antarctica* (Prymnesiophyceae) colonies in the Ross Sea, Antarctica. Journal of Phycology 36, 1–8.

Mclntyre, S., Alldredge, A.L., Gotschalk, C.C., 1998. Accumulation of marine snow at density discontinuities in the water column. Limnology and Oceanography 40 (3), 449–468.

Passow, U., Wassmann, P., 1994. On the trophic fate of *Phaeocystis pouchetii* (Hariot): IV. The formation of marine snow by *P. pouchetii*. Marine Ecological Progress 104, 153–161.

Passow, U., Alldredge, A.L., Logan, B.E., 1994. The role of particulate carbohydrate exudates in the flocculation of diatom blooms. Deep-Sea Research I 41, 335–357.

Pilskaln, C.H., Lehmann, C., Paduan, J.B., Silver, M.W., 1998. Spatial and temporal dynamics in marine aggregate abundance, sinking rate and flux: Monterey Bay, central California. Deep-Sea Research I 45, 1803–1838.

Riebesell, U., 1991. Particle aggregation during a diatom bloom. I. Physical aspects. Marine Ecological Progress 69, 273–280.

Riebesell, U., 1993. Aggregation of *phaeocystis* during phytoplankton spring blooms in the southern North Sea. Marine Ecological Progress 96, 281–289.

Riebesell, U., Wolf-Gladrow, D.A., 1992. The relationship between physical aggregation of phytoplankton and particle flux: a numerical model. Deep-Sea Research 39, 1085–1102.

Smith Jr., W.O., Nelson, D.M., 1985. Phytoplankton bloom produced by a receding ice edge in the Ross Sea: spatial coherence with the density field. Science 227, 163–166.

Smith Jr., W.O., Dunbar, R.B., 1998. The relationship between new production and vertical flux on the Ross Sea continental shelf. Journal of Marine Systems 17, 445–457.

Smith Jr., W.O., Asper, V.A., 2001. The influence of phytoplankton assemblage composition on biogeochemical characteristics and cycles in the southern Ross Sea, Antarctica. Deep-Sea Research I 48, 137–161.

Smith Jr., W.O., Nelson, D.M., DiTullio, G.R., Leventer, A.R., 1996. Temporal and spatial patterns in the Ross Sea: phytoplankton biomass, elemental composition, productivity and growth rates. Journal of Geophysical Research 101, 18455–18466.

Smith Jr., W.O., Marra, J., Hiscock, M.R., Barber, R.T., 2000. The seasonal cycle of phytoplankton biomass and primary productivity in the Ross Sea, Antarctica. Deep-Sea Research II 47, 3119–3140.

Sweeney, C., Hansell, D.A., Millero, F.D., Takahashi, T., Gordon, L.I., Carlson, C.A., Codispoti, L.A., Smith Jr., W.O., Marra, J., 2000. Biogeochemical regimes, net community production and carbon export in the Ross Sea, Antarctica. Deep-Sea Research II 47, 3369–3394.

Tiselius, P., Kuylenstierna, M., 1996. Growth and decline of a diatom spring bloom: phytoplankton species composition, formation of marine snow and the role of heterotrophic dinoflagellates. Journal of Plankton Research 18, 133–155.

Trent, J.D., Shanks, A.L., Silver, M.W., 1978. In situ and laboratory measurements on macroscopic aggregates in Monterey Bay, California. Limnology and Oceanography 23, 626–636.

Waite, A., Gallager, S., Dam, H.G., 1997. New measurements of phytoplankton aggregation in a flocculator using videography and image analysis. Marine Ecological Progress 155, 77–88.

Zwally, H.J., Comiso, J.C., Parkinson, C.L., Campbell, W.J., Carsey, F.D., Gloersen, P., 1983. Antarctic sea ice, 1973–1976: Satellite passive-microwave observations. NASA Special Publication NASA SP-459, 206pp.